$$A_{20}\left(\varphi, \frac{\pi}{2}\right) = -\frac{1}{2}A_{20}(0) + \frac{\sqrt{6}}{2}\cos(2\varphi)A_{22}(0) \tag{5.19a}$$

$$A_{2\pm2}\left(\varphi, \frac{\pi}{2}\right) = \frac{\sqrt{6}}{4}A_{20}(0) + \frac{1}{2}\cos(2\varphi)A_{22}(0) \tag{5.19b}$$

The last equation infers that the absorber matrices are diagonal with respect to the systems S^γ. The r matrices are given by (the argument $\vartheta = 0$ is dropped)

$$\mathbf{k}\|c, \qquad \bar{r}_{xx,yy}(0, 0) = \frac{1}{2} + gA_{20} \pm \sqrt{6}hA_{22} \tag{5.20a}$$

$$\mathbf{k}\|b, \qquad \bar{r}_{xx,yy}\left(0, \frac{\pi}{2}\right) = \frac{1}{2} + g\left(-\frac{1}{2}A_{20} + \frac{\sqrt{6}}{2}A_{22}\right) \pm h\left(\frac{3}{2}A_{20} + \frac{\sqrt{6}}{2}A_{22}\right) \tag{5.20b}$$

$$\mathbf{k}\|a, \qquad \bar{r}_{xx,yy}\left(\frac{\pi}{2}, \frac{\pi}{2}\right) = \frac{1}{2} + g\left(-\frac{1}{2}A_{20} - \frac{\sqrt{6}}{2}A_{22}\right) \pm h\left(\frac{3}{2}A_{20} - \frac{\sqrt{6}}{2}A_{22}\right) \tag{5.20c}$$

The evaluation of the three Mössbauer spectra of SNP has been done by the following evaluation procedure. In the beginning the absorber is considered as unpolarized. The fractional polarization $a = (\bar{r}_{xx} - \bar{r}_{yy})/(\bar{r}_{xx} + \bar{r}_{yy})$ is set to zero. Inserting $a = 0$, and the reduced areas $A^i \cdot 2/(\Gamma\pi) \cdot 1/f_s$ of the separated absorption lines $i = l, h$ into equation (5.12b), a first approximation of the average cross section $\bar{\sigma}^{l,h}$ of each line is obtained. Lines l and h are the low and high velocity lines, respectively. With $t = \bar{\sigma}^l + \bar{\sigma}^h$ the traces of the $\bar{r}$ matrices $\bar{r}^i_{xx} + \bar{r}^i_{yy} = 2\bar{\sigma}^i/t$ of the two lines are determined. According to equation (5.20) the traces of the three directions are given by

$$(\bar{r}^i_{xx} + \bar{r}^i_{yy})_c = 1 + 2gA^i_{20} \tag{5.21a}$$

$$(\bar{r}^i_{xx} + \bar{r}^i_{yy})_b = 1 - gA^i_{20} + g\sqrt{6}A^i_{22} \tag{5.21b}$$

$$(\bar{r}^i_{xx} + \bar{r}^i_{yy})_a = 1 - gA^i_{20} - g\sqrt{6}A^i_{22} \tag{5.21c}$$

The subscripts (a,b,c) denote the axes being parallel to the γ-direction. Two of these equations already determine A^i_{20} and A^i_{22}. With the values of A^i_{20} and A^i_{22} the fractional polarization $a^i = (\bar{r}^i_{xx} - \bar{r}^i_{yy})/(\bar{r}^i_{xx} + \bar{r}^i_{yy})$ is

calculated, which will be now different from zero. Here the calculation of the a^i is very simple because the r matrices are already diagonal. The second step uses the value a^i in equation (5.12b) to obtain improved values of the average cross sections $\bar{\sigma}^i$. After a few steps this procedure converges. For the SNP absorber Grant *et al.*[5] would have obtained ($g = h = 1$)

$$A_{20}^{l,h} = \pm 0.1237, \qquad A_{22}^{l,h} = \mp 0.0462 \tag{5.22}$$

In addition the f factors (f_a, f_b, f_c) parallel to the crystallographic axes are known from the effective thickness (t_a, t_b, t_c). It should be noted that this procedure is only applicable for $g(\delta) \neq 0$. In the case of ^{197}Au the small absolute value of $g = -0.305$ makes an accurate determination of the A_{2m}^i more difficult.

5.2.1b. The EFG Tensor of Sodium Nitroprusside. The evaluation of the EFG tensor has been described in detail in Section 4.2.1. The traceless tensor $\bar{T}_{ik}$ is defined by equation (4.40). Inserting the A_{20} and A_{22} tensor component of equation (5.22) we obtain

$$\bar{T}_{xx}^h = 0.118, \qquad \bar{T}_{yy}^h = 0.005, \qquad \bar{T}_{zz}^h = -0.124 \tag{5.23}$$

In accordance with the orthorhombic symmetry of the crystal the non-diagonal elements of the average of the traceless tensor vanish (i.e., $\bar{T}_{xy} = \bar{T}_{xz} = \bar{T}_{yz} = 0$). The invariants $T_\Delta = 64\phi_{II}(T_{pq})$ of a single lattice site ($T_\Delta = 1$) and of the average tensor $T_\Delta{}^m$ have led to equation (4.44), which is now given by

$$L^2 = (T_{xy}^h)^2 + (T_{xz}^h)^2 + (T_{yz}^h)^2 = \frac{3}{64}(1 - T_\Delta{}^m) \tag{5.24}$$

where $(3/64)(1 - T_\Delta{}^m) = 0.0322$. In analogy to equation (4.49) the components $T_{ik}(i \neq k)$ of the local tensor can be expressed by two angles Θ, Ψ and $L = 0.179$:

$$\begin{aligned} T_{xy}^h &= L \sin\Theta \cos\Psi, \qquad T_{xz}^h = L \sin\Theta \sin\Psi \\ T_{yz}^h &= L \cos\Theta \end{aligned} \tag{5.25}$$

The general case of an orthorhombic crystal leaves a two-parameter manifold. The Euler angles α, β, γ and the asymmetry parameter η are parametrized by the two angles Θ, Ψ. It is noted that this procedure is applicable for any $3/2 \rightarrow 1/2$ transition including those of mixed type [$g(\delta)$

and $h(\delta)$ do not appear in the equations above]. The special symmetry of SNP, however, yields a unique solution. The fact that the iron atoms lie on mirror planes requires one principal axis of the EFG being parallel to the crystallographic c axis. The tensor components T^h_{xz} and T^h_{yz} vanish, so that T^h_{xy} is determined by equation (5.24) to be $T^h_{xy} = \pm L$. The invariant $T_\eta = 256\phi_{III}(T^h_{pq}) = 0.999$ determines the sign of V_{zz} to be positive [equation (4.51)] and the asymmetry parameter [equation (4.52)] to be close to zero ($\eta \sim 0$). Diagonalizing the tensor T^h, which is proportional to the EFG tensor, we see that the z axes of the two equivalent sites lie in the a,b plane rotated by $\alpha = \pm 34°$ out of the a,c plane. The x axes are parallel to the c axis. This result is in agreement with that of Grant *et al.*[5] Here the data could be evaluated in a straightforward manner by the tensor method as compared to the complicated argumentation in the work of Grant *et al.*[5]

We will also evaluate the data by the direct use of the A_{2m}-tensor components. This procedure, which is applicable to any transition, has been described in the beginning of Section 4.2.1. For the $3/2 \rightarrow 1/2$ transition the expressions of the A_{2m} are already explicitly calculated in the case of a monoclinic crystal. It is easily seen that equation (4.42) can also be used for orthorhombic symmetry. Two equivalent sites, one of them having the orientation $\boldsymbol{\beta} = (\alpha, \beta, \gamma)$, are related by the twofold axis parallel $\mathbf{e}^C_z$. The tensor components A_{2m} of the monoclinic symmetry belong to these two sites. The two other equivalent sites of the orthorhombic crystal are obtained by the twofold rotation C_{2x} (or C_{2y}), so that the components A'_{2m} belonging to the new sites are $A'_{2m} = \Sigma_n A_{2n} D^2(C_{2x})_{nm}$, which gives [equation (3.98)] $A'_{2m} = A_{2-m}$. Consequently the averages representing the orthorhombic structure A_{2m} (orthorhombic) $= \frac{1}{2}(A'_{2m} + A_{2m})$ are the same for A_{20} and $A_{22} + A_{2-2}$ of the monoclinic structure. The average of $A_{22} - A_{2-2}$ vanishes. So we can use equation (4.42a) and (4.42b) depending on the parameters η, $\boldsymbol{\beta}$. The special symmetry at the iron sites restrict $\boldsymbol{\beta}$ to $\boldsymbol{\beta} = (0, 0, \gamma)$, (the V_{zz} axis is parallel to the c axis) and $\boldsymbol{\beta} = (\alpha, \pi/2, 0)$, (the V_{zz} axis lies in the a,b plane). $\boldsymbol{\beta} = (\alpha, 0, 0)$ can be immediately excluded by equation (4.42a):

$$A^\pi_{20} = \frac{1}{4(1 + \eta^2/3)^{1/2}} \neq A^{h,l}_{20} = \pm 0.1237 \tag{5.26}$$

independent of the value of η. The second solution is given by

$$A^\pi_{20} = -\tfrac{1}{8}(1 - \eta)/(1 + \eta^2/3)^{1/2} \tag{5.27a}$$

$$\frac{\sqrt{6}}{4}(A^\pi_{22} + A^\pi_{2-2}) = \frac{1}{16}(3 + \eta)\cos(2\alpha)/(1 + \eta^2/3)^{1/2} \tag{5.27b}$$

From the sign of A_{20}^{π} we conclude that the high-velocity line is the π transition ($A_{20}^{\pi} = A_{20}^{h}$), so that $V_{zz} > 0$ and $\eta = 0.01$. The second equation determines α to be $\pm$ 36°.

5.2.1c. The MSD Tensor of Sodium Nitroprusside. It has already been mentioned (Section 3.4.3) that for low γ energies the molecular f factor f_M is isotropic to a good approximation.[38] Then the PAS of the MSD tensor of an orthorhombic crystal coincides with the crystal axes. Grant *et al.*[5] measured the PAS of the MSD tensor in SNP. The mirror plane at the iron sites requires the c axis to be one principal axis of the MSD tensor. One measurement in the a,b plane is therefore sufficient to determine the complete PAS.

In order to construct the absorber matrix we start with the average of the tensors $A_{Lm}(i)$ of site i [equation (3.118b)]:

$$A_{Lm} = \frac{1}{n} \sum_{i=1}^{n} A_{Lm}(i) f(S^E, \beta_i)/\bar{f} \tag{5.28}$$

$n = 4$ is the number of equivalent sites. Since the direction of observation is normal to the twofold z axis the f factor is the same for the pairs of sites [for instance: (1,2) = u and (3,4) = v] related by this twofold rotation. The sum in equation (5.29) can be rearranged so that

$$A_{Lm} = \tfrac{1}{2}[A_{Lm}(u) f(u) + A_{Lm}(v) f(v)]/\bar{f} \tag{5.29a}$$

where $\bar{f} = [f(u) + f(v)]/2$ is the average of the f factors of pair u and pair v. The $A_{Lm}(u)$ and $A_{Lm}(v)$ are the tensor components of a monoclinic crystal. They are given with respect to the system S^{γ}, which is rotated out of the system S^{C} by the Euler angles $\vartheta = (\varphi, \pi/2, 0)$. Equation (5.29) depends on the variable φ. Explicitly we have ($L = 2$)

$$A_{2m}(\varphi) = \tfrac{1}{2}[A_{2m}(u,\varphi) f(u,\varphi) + A_{2m}(v,\varphi) f(v,\varphi)]/\bar{f}(\varphi) \tag{5.29b}$$

By use of the transformation property equation (3.79) the $A_{2m}(u, \varphi)$ are expressed by the $A_{2m}(u, \vartheta = 0) \equiv A_{2m}$:

$$A_{20}(u, \varphi) = -\frac{1}{2} A_{20} + \frac{\sqrt{6}}{4} \cos(2\varphi)(A_{22} + A_{2-2}) + \frac{\sqrt{6}}{4} \sin(2\varphi) i (A_{22} - A_{2-2})$$

$$A_{22}(u, \varphi) = \frac{\sqrt{6}}{4}A_{20} + \frac{1}{4}\cos(2\varphi)(A_{22} + A_{2-2}) \qquad (5.30)$$

$$+ \frac{1}{4}\sin(2\varphi)i(A_{22} - A_{2-2})$$

$$A_{2-2}(u, \varphi) = A_{22}(u, \varphi)$$

The v sites are related to the u sites by a C_{2x} rotation. The same holds for the tensor components so that $A_{2m}(u, \vartheta = 0) = A_{2-m}(v, \vartheta = 0)$ (see the preceding section). Inserting these relations into equation (5.30) we obtain

$$A_{20}(\varphi) = -\frac{1}{2}A_{20} + \frac{\sqrt{6}}{4}\cos(2\varphi)(A_{22} + A_{2-2})$$

$$+ \frac{\sqrt{6}}{8}\sin(2\varphi)i(A_{22} - A_{2-2})[f(u, \varphi) - f(v, \varphi)]/\bar{f}(\varphi)$$

$$A_{22}(\varphi) = \frac{\sqrt{6}}{4}A_{20} + \frac{1}{4}\cos(2\varphi)(A_{22} + A_{2-2}) \qquad (5.31)$$

$$+ \frac{1}{8}\sin(2\varphi)i(A_{22} - A_{2-2})[f(u, \varphi) - f(v, \varphi)]/\bar{f}(\varphi)$$

$$A_{2-2}(\varphi) = A_{22}(\varphi)$$

The following comment on this equation is useful. We know that the orthorhombic structure only reveals the tensor components A_{20} and $\frac{1}{2}(A_{22} + A_{2-2}) = A_{2\pm2}$ (orthorhombic) if the f factor f_M is isotropic. For an anisotropic f factor f_M the measurements contain information of the other components of the A_{Lm} tensor but connected with the orientation dependence of the f factors at each site. This property is reflected by the infinite series of the super-texture components, the use of which has been avoided above. In our case the quantity

$$\Delta(\varphi) = -i\frac{\sqrt{6}}{8}(A_{22} - A_{2-2})[f(u, \varphi) - f(v, \varphi)]/\bar{f}(\varphi) \qquad (5.32)$$

is determined.

For the special symmetry at the iron sites the factor $T_{xy} = -i\cdot(\sqrt{6}/4)(A_{22} - A_{2-2})$ is already evaluated in equation (4.38c). The Euler angles $\boldsymbol{\beta} = (\alpha, \pi/2, 0)$ give

$$-i\frac{\sqrt{6}}{4}(A_{22} - A_{2-2}) = -\frac{1}{16}(3 + \eta)\sin(2\alpha)/(1 + \eta^2/3)^{1/2} \quad (5.33)$$

The pairs of sites related by the C_{2z} axis have the same orientation, so that there is just one site u and v, the orientation of their EFG tensors being $\boldsymbol{\beta} = (\alpha = \pm 36°, \pi/2, 0)$ and their f factors being related by the equation $f(v, \varphi) = f(u, \varphi)$. At $\varphi = 0$ and $\varphi = \pi/2$ the f factors are

$$f(u, 0) = f(v, 0) = f_a \quad \text{and} \quad f(u, \pi/2) = f(v, \pi/2) = f_b$$

Grant *et al.*[5] measured at $\varphi = 54°$ and found that the value of Δ vanishes within the experimental error so that $f(u, 54°) = f(v, -54°)$. Consequently the a axis is a twofold symmetry axis of the MSD tensor and the PAS of the MSD tensors at site u and v are identical and coincide with the crystal axes. An anisotropic molecular f factor f_M could not be detected in this compound.

5.2.1d. The Intensity Matrix of Sodium Nitroprusside. Finally we will show that for the pure dipole (multipole) transitions the absorber matrices are more easily calculated by use of the intensity matrix.[11,15] For this purpose the matrix I^π of equation (3.60) is transformed from the spherical basis to the real basis $\mathbf{e}_x, \mathbf{e}_y, \mathbf{e}_z$ (the superscript $L = 1$ is dropped):

$$I^\pi = \begin{pmatrix} \frac{1}{4}(e_- - \sqrt{3}\, e_+)^2 & & \\ & \frac{1}{4}(e_- + \sqrt{3}\, e_+)^2 & \\ & & e_-^2 \end{pmatrix},$$

$$I^\sigma = 1_3 - I^\pi \quad (5.34)$$

Inserting the $e_\pm$ values of equation (2.4) we have explicitly

$$I^\pi = \frac{1}{2} + \frac{1}{2\sqrt{1 + \eta^2/3}} \begin{pmatrix} (1 - \eta)/2 & & \\ & (1 + \eta)/2 & \\ & & -1 \end{pmatrix} \quad (5.35)$$

Comparing this matrix with the traceless intensity tensor T^π [equation (4.44)] we find again $I^\pi = \frac{1}{2}1_3 - 2T^\pi$ of equation (5.17). The intensity matrix with respect to the crystal system S^C is obtained by the transformation

$$I^\pi(S^C) = R^{-1}(\boldsymbol{\beta})I^\pi(S^E)R(\boldsymbol{\beta}) \quad (5.36)$$

$R(\boldsymbol{\beta})$ rotates S^C to S^E. In the special case of the SNP crystal the R matrixes of the two sites are ($\alpha = 36°$)

$$R(\pm\alpha,\ \pi/2,\ 0) = \begin{pmatrix} 0 & 0 & -1 \\ \mp\sin\alpha & \cos\alpha & 0 \\ \cos\alpha & \pm\sin\alpha & 0 \end{pmatrix} \tag{5.37}$$

The nonzero intensity matrix elements with respect to the system S^C of the two sites are calculated to be

$$\begin{aligned} I^{\pi}_{xx}(\pm\alpha) &= \tfrac{1}{2} - \tfrac{1}{8}[(1-\eta) + (3+\eta)\cos(2\alpha)]/(1+\eta^2/3)^{1/2} \\ I^{\pi}_{yy}(\pm\alpha) &= \tfrac{1}{2} - \tfrac{1}{8}[(1-\eta) - (3-\eta)\cos(2\alpha)]/(1+\eta^2/3)^{1/2} \\ I^{\pi}_{zz}(\pm\alpha) &= \tfrac{1}{2} + \tfrac{1}{4}(1-\eta)/(1+\eta^2/3)^{1/2} \\ I^{\pi}_{xy}(\pm\alpha) &= \mp\tfrac{1}{8}(3+\eta)\sin(2\alpha)/(1+\eta^2/3)^{1/2} \end{aligned} \tag{5.38}$$

The absorber matrix elements $r_{ik} = I_{ik}$ for the different directions are again obtained by the transformation of I_{ik}. Instead of the transformation we can also directly write (similarly as for the tensor T_{ik} in equation (4.43)]

$$r_{ik}(\vartheta) = \mathbf{e}^{\gamma}_i(\vartheta) I(S^C) \mathbf{e}^{\gamma}_k(\vartheta), \qquad i = x,y \tag{5.39}$$

$\mathbf{e}^{\gamma}_x$ and $\mathbf{e}^{\gamma}_y$ are the polarization vectors. At first we consider the three γ directions parallel to the twofold crystal axes. The absorber matrix elements are always a pair of the diagonal elements of I. We have for example for $\mathbf{e}^{\gamma}_z = \mathbf{e}^{C}_x$ the absorber matrix elements $r_{xx} = I_{yy}$, $r_{yy} = I_{zz}$. Since the trace of I is 3/2, two parameters determine the intensity of the three directions in agreement with the number of independent tensor components A_{Lm} of the orthorhombic crystal (A_{20}, A_{22}). Both sites ($\pm\alpha$) give the same contribution. For an arbitrary γ direction $\mathbf{e}^{\gamma}_z = (\cos\varphi, \sin\varphi, 0)$ in the a,b plane the off-diagonal element I_{xy} is also involved. With $\mathbf{e}^{\gamma}_x = \mathbf{e}^{C'}_z = (0, 0, 1)$ the vector $\mathbf{e}^{\gamma}_y = \mathbf{e}^{\gamma}_z \times \mathbf{e}^{\gamma}_x$ becomes $\mathbf{e}^{\gamma}_y = (\sin\varphi, -\cos\varphi, 0)$. The absorber matrix is then given by

$$\begin{aligned} r_{xx}(\alpha,\ \varphi) &= I_{zz}(\alpha) \\ r_{yy}(\alpha,\ \varphi) &= \tfrac{1}{2}[I_{xx}(\alpha) + I_{yy}(\alpha)] + \tfrac{1}{2}[I_{yy}(\alpha) - I_{xx}(\alpha)]\cos(2\varphi) \\ &\quad - I_{xy}(\alpha)\sin(2\varphi) \\ r_{xy}(\alpha,\ \varphi) &= r_{yx}(\alpha,\ \varphi) = 0 \end{aligned} \tag{5.40}$$

The averages of the absorber matrices of both sites u and v are finally given by

$$\bar{r}_{ik}(\varphi) = \tfrac{1}{2}[r_{ik}(\alpha,\ \varphi) f(u,\ \varphi) + r_{ik}(-\alpha,\ \varphi) f(v,\ \varphi)]/\bar{f}(\varphi) \tag{5.41}$$

Zimmermann[54] introduced another tensor of the cofactors of T_{ik}. This tensor allows us to calculated the square of the polarization $a^2 = (r_{xx} - r_{yy})^2/(r_{xx} + r_{yy})^2$ directly using the components of the unit vector $\mathbf{e}_z^\gamma$. The polarization vectors $\mathbf{e}_{x,y}^\gamma$ need not be considered and the r matrix does not need to be diagonalized. If, however, the polarization vectors can be easily chosen so that r is diagonal, the introduction of this tensor finally does not simplify the calculation and is therefore not described here.

5.2.2. *The Intensity Matrix of the Mohr Salt (^{57}Fe)*

The Mohr salt $(NH_4)_2{\cdot}Fe(SO_4)_2{\cdot}6H_2O$ has monoclinic crystal symmetry. The two equivalent iron sites per unit cell are related by the twofold axis b. The z axis of the system S^C is chosen to be parallel to the b axis and the x axis parallel to the c axis. The intensity matrix of the crystal with respect to S^C

$$I = \begin{pmatrix} I_{xx} & I_{xy} & 0 \\ I_{yx} & I_{yy} & 0 \\ 0 & 0 & I_{zz} \end{pmatrix} \tag{5.42}$$

has three independent parameters: I_{xx}, I_{yy}, $I_{xy} = I_{yx}$. I_{zz} is given by the $\mathrm{Tr}(I) = 3/2$. The macroscopic matrix can be defined for the γ direction parallel and normal to the twofold axis b, where the f factors of both sites are the same. The absorber matrix of the γ direction $\mathbf{e}_z^\gamma = (\cos\varphi, \sin\varphi, 0)$ in the a,b plane has already been calculated considering the matrix of SNP. The diagonal matrix is given by equation (5.41). For $\mathbf{k} \parallel b$ axis the absorber matrix

$$r = \begin{pmatrix} I_{xx} & I_{xy} \\ I_{yx} & I_{yy} \end{pmatrix} \tag{5.43}$$

has to be diagonalized to calculate the fractional polarization a used for the iteration procedure described in Section 5.2.1a. One easily obtains

$$a = [(I_{xx} - I_{yy})^2 + 4I_{xy}^2]^{-1/2}/(I_{xx} + I_{yy}) \tag{5.44}$$

From three measurements, one parallel to the b axis and two in the a,c plane at $\varphi = 47.6°$ normal to the $\bar{2}01$ plane and $\varphi = -17°$ normal to the 010 plane, the traceless intensity matrix $T_{ik} = \frac{1}{2}(\frac{1}{2}\delta_{ik} - I_{ik})$ was determined.[54] The principal values of the tensor of the high-velocity line are

$$T_{\xi\xi}^h = 0.191, \qquad T_{\eta\eta}^h = -0.227, \qquad T_{\varphi\varphi}^h = 0.036 \tag{5.45}$$

The error is about 0.004. The φ axis is parallel to the z axis and the ξ axis is rotated by 34.5° towards the a axis.

This result will be referred to in the next section. The manifold of solutions of the EFG tensors obtained from the tensor T_{ik} will not be discussed here.

5.3. A Polarized Source

A polarized source is as shown in the beginning very helpful for the determination of the r matrix of an absorption line. In the case of ^{57}Fe a polarized source is obtained by ^{57}Co in a magnetized iron foil. Several measurements on magnetically split absorbers have been done by Gonser *et al.*[26] Here a measurement of Gibb[55] is presented where the polarization of the transmitted beam, which is originally unpolarized, is used as a polarized source.[56] T.C. Gibb[55] performed a Mössbauer measurement with two single crystals of the Mohr salt $Fe(NH_4)_2(SO_4)_2{\cdot}6H_2O$. The crystal plates of the monoclinic crystals were cut parallel to the $(\bar{2}01)$ plane which contains the twofold b axis. So the γ direction was normal to the b axis (Figure 12) and at an angle of 47.3° to the c axis in the a,c plane. The Mössbauer spectra are measured for different relative orientations of the two crystals which have the same γ direction but are rotated by an angle ψ against each other. Instead of the result of Gibb for the EFG tensor at the Fe sites we use the intensity tensor which was precisely remeasured by Zimmermann and Dörfler[54] (see Section 5.2.2). From their traceless intensity tensor [equation (5.46)] the intensity matrix is obtained:

$$I^h_{\xi\xi} = 0.118, \qquad I^h_{\eta\eta} = 0.954, \qquad I^h_{\zeta\zeta} = 0.428 \tag{5.46}$$

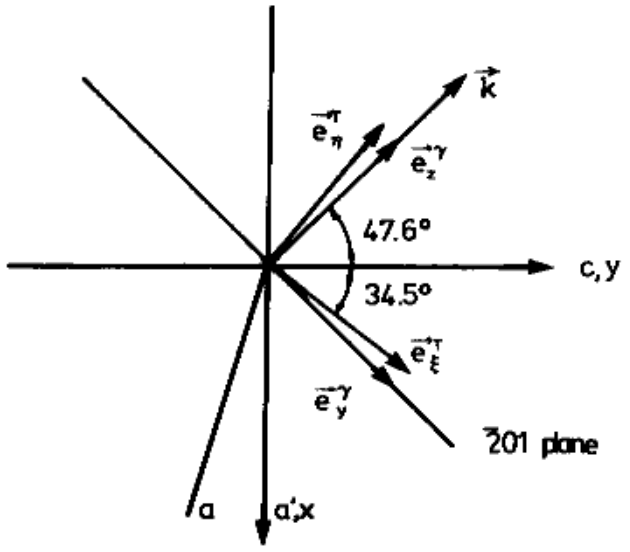

FIGURE 12. The projection of the crystal structure of $Fe(NH_4)_2(SO_4)_2{\cdot}6H_2O$ on the a,c plane is shown. The γ direction $\mathbf{k}$ is normal to the $\bar{2}01$-plane. The axes system $(\mathbf{e}^I_i)$ is the PAS of the intensity tensor. The twofold b axis is normal to the a,c plane and coincides with the vectors $\mathbf{e}^I_\xi$ and $\mathbf{e}^\gamma_y$.

List of Symbols

$A_i^{\alpha\beta}$	absorption area of the transition (α, β) and source line i
A_{Lm}	tensor components
a_m^L	see equation (3.78)
AS	axes system
$\boldsymbol{\beta}$	$\equiv (\alpha, \beta, \gamma)$ (Euler angles)
d	thickness of the absorber
$d^L_{m'm}(\vartheta)$	rotation matrix
E_α	energies of the nuclear ground states
E_β	energies of the excited nuclear states
EFG	electric field gradient
$\mathbf{e}_i$	unit vectors ($i = x,y,z$)
η	asymmetry parameter of the EFG
$f(\vartheta)$	Debye–Waller factor
f_m^L	expansion coefficient of the Debye–Waller factor
f_s	Debye–Waller factor of the source
$(I^L_{pq})^{\alpha\beta}$	intensity matrix of the pure multipole (L) transition (α, β)
$J_{pq}^{\alpha\beta}$	interference matrix ($M1/E2$)
$\mathbf{k}$	wave vector
MSD	mean square displacement
n	(i) index of refraction (2×2 matrix) (ii) asymmetry parameter of an orthorhombic MSD tensor
ν	$\equiv -ikd(n^+ - n)$ (Hermitian 2×2 matrix)
N	(i) asymmetry parameter of an axial MSD tensor (ii) number of Mössbauer nuclei per unit volume
PAS	principal axes system
$\mathbf{P}$	Poincaré vector
ϕ_i	i = I,II,III; invariants of a second-rank tensor
Q	quadrupole moment
$f^{\alpha\beta}$	absorber matrix of the transition (α, β)
$\bar{f}^{\alpha\beta}$	average absorber matrix
ρ	density matrix
S^A	AS of the absorber
S^C	AS of the crystal
S^γ	AS defined with respect to the laboratory with $\mathbf{k} \parallel z$ axis
S^E	PAS of the EFG tensor
S^M	PAS of the MSD tensor
$\sigma^{\alpha\beta}$	$= f^{\alpha\beta}\cdot t$
$\mathrm{SP}(v)_i^{\alpha\beta}$	spectrum of the transition (α, β) and source line i
SP(v)	total spectrum
t	effective thickness of the absorber

$T(\beta)$	texture function
$t^L_{m'm}$	texture parameter
θ	$\equiv (\phi, \theta, \Psi)$ (Euler angles)
ϑ	$\equiv (\varphi, \vartheta, \psi)$ (Euler angles)
$\theta^L_{m'm}$	super-texture components
V_{ik}	$i,k = x,y,z$, components of the EFG tensor
ζ	$\equiv f^0_0/\exp[-\frac{1}{3}k^2(\langle x^2\rangle + \langle y^2\rangle + \langle z^2\rangle)]$
ζ^L_m	$\equiv f^L_m/f^0_0$
$\zeta^L_{M,m}$	$\equiv f^L_{M,m}/f^0_{M,0}$ (molecular part)
$\zeta^L_{C,m}$	$\equiv f^L_{C,m}/f^0_{C,0}$ (lattice part)

References

1. H. Frauenfelder, D.E. Nagle, R.D. Taylor, D.R.F. Cochran, and W.M. Visscher, *Phys. Rev.* **126,** 1065 (1962).
2. M. Blume and O.C. Kistner, *Phys. Rev.* **171,** 417 (1968).
3. R.M. Housley, R.W. Grant, and U. Gonser, *Phys. Rev.* **178,** 514 (1969).
4. R. Zimmermann, *Nucl. Instrum. Methods* **128,** 537 (1975).
5. R.W. Grant, R.M. Housley, and U. Gonser, *Phys. Rev.* **178,** 523 (1969).
6. Y. Maeda, T. Harami, A. Trautwein, and U. Gonser, *Z. Naturforsch.* **31b,** 487 (1976).
7. F. Parak, U.F. Thomanek, D. Bade, and B. Wintergerst, *Z. Naturforsch.* **32c,** 507 (1977).
8. M. Grodzicki, S. Lauer, and A.X. Trautwein, in *Mössbauer Spectroscopy and its Chemical Applications,* J.G. Stevens and G.K. Shenoy eds., Advances in Chemistry Series No. 194, American Chemical Society, Washington, D.C., 1981, p. 3.
9. R. Zimmerman, *Chem. Phys. Lett.* **34,** 416 (1975).
10. Alumuddin, A. Lal, and K. Rama Reddy, *Nuovo Cimento* **32B,** 389 (1976).
11. H. Spiering, *Hyperfine Interactions* **3,** 213 (1977).
12. R.M. Steffen and K. Alder, in *The Electromagnetic Interaction in Nuclear Spectroscopy,* W.D. Hamilton, ed., North-Holland, Amsterdam, 1975.
13. U. Gonser and H.D. Pfannes, *J. Phys. (Paris)* **35,** C6-113 (1974).
14. H.D. Pfannes and H. Fischer, *Appl. Phys.* **13,** 317 (1977).
15. H. Spiering and H. Vogel, *J. Phys. (Paris)* **40,** C2-50 (1979).
16. M. Rots, R. Coussement, J. Claes, and L. Hermans, *Hyperfine Interactions* **11,** 185 (1981).
17. V.I. Goldanskii, G.M. Gorodinskii, S.V. Karyagin, L.A. Korytko, L.M. Krizhanskii, E.F. Makarov, I.P. Suzdalev, and V.V. Khrapov, *Proc. Acad. Sci. USSR, Phys. Chem. Sect.* **147,** 766 (1963).
18. S.V. Karyagin, *Dokl. Akad. Nauk. SSSR* **148,** 1102 (1963).
19. A. Abragam and B. Bleaney, *Electron Paramagnetic Resonance of Transition Ions,* Clarendon Press, Oxford, 1970.
20. P.G.L. Williams and G.M. Bancroft, in *Mössbauer Effect Methodology,* I.J. Gruverman, ed., Plenum Press, New York, 1971, Vol. 7, p. 39.
21. P. Zory, *Phys. Rev.* **140,** A1401 (1965).

22. S. Kareem, M. Ali, Alumuddin, and R.K. Tyagi, Proc. of the International Conference on the Application of the Mössbauer Effect, Jaipur, India, 1981, p. 583.
23. C.L. Chein, S. De Benedetti, and F. de S. Barros, *Phys. Rev. B* **10,** 3913 (1974).
24. P. Imbert, *Phys. Lett.* **8,** 95 (1964).
25. R.M. Housley and U. Gonser, *Phys. Rev.* **171,** 480 (1968).
26. U. Gonser and H. Fischer, in *Mössbauer Spectroscopy II,* U. Gonser, ed., Springer-Verlag, Berlin, 1981, p. 49.
27. U. Fano, *Rev. Mod. Phys.* **29,** 74 (1957).
28. M.E. Rose, *Elementary Theory Of Angular Momentum,* John Wiley, New York, 1957.
29. M. Lax, *Rev. Mod. Phys.* **126,** 1045 (1962).
30. G.T. Trammell, *Phys. Rev.* **126,** 1045 (1962).
31. G.T. Trammell and J.P. Hannon, *Phys. Rev.* **180,** 337 (1969).
32. A.M. Afanas'ev and Y. Kagan, *Phys. Lett.* **31a,** 38 (1970).
33. D.L. Nagy, *Appl. Phys.* **17,** 269 (1978).
34. H. Prosser, F.E. Wagner, G. Wortmann, and G.M. Kalvius, *Hyperfine Interactions* **1,** 25 (1975).
35. J.M. Greneche and F. Varret, *J. Phys. (Paris) Lett.* **43,** L233 (1982).
36. T. Ericson and R. Wappling, *J. Phys. (Paris)* **37,** C6-719 (1976).
37. U. Gonser, *J. Phys. Chem.* **66,** 564 (1962).
38. R. Chandra and T. Ericsson, *Hyperfine Interactions* **7,** 229 (1979).
39. C.L. Chien and A.W. Sleight, *Phys. Rev. B* **18,** 2031 (1978).
40. V.I. Goldanskii and E.F. Makarov, in *Chemical Applications of Mössbauer Spectroscopy,* V.I. Goldanskii and R.H. Herber, eds., p. 105, Academic Press, New York, 1968.
41. E.R. Bauminger, A. Diamant, I. Felner, I. Nowik, and S. Ofer, *Phys. Lett.* **50A,** 321 (1974).
42. H. Armon, E.R. Bauminger, A. Diamant, I. Nowik, and S. Ofer, *Solid State Commun.* **15,** 543 (1974).
43. M.O. Faltens and D.A. Shirley, *J. Chem. Phys.* **53,** 4249 (1970).
44. H.D. Bartunik, W. Potzel, R.L. Mössbauer, and G. Kaindl, *Z. Phys.* **240,** 1 (1970).
45. J. Danon, in *Mössbauer Spectroscopy and its Applications,* IAEA, Vienna, 1972.
46. A. Rosencwaig and D.T. Cromer, *Acta Crystallogr.* **12,** 704 (1959).
47. M.T. Hirvonen, A.P. Jauho, T.E. Katila, J.A. Pohjonen, and K.J. Riski, *J. Phys. (Paris)* **37,** C6-501 (1976).
48. W. Keune, S.K. Date, I. Dèzsi, U. Gonser, *J. Appl. Phys.* **46,** 3914 (1975).
49. G.A. Bykow, P.Z. Hien, *Sov. Phys. JETP* **16,** 646 (1963).
50. H. Spiering and H. Vogel, *Hyperfine Interactions* **3,** 221 (1977).
51. A.J. Stone, *Nucl. Instrum. Methods* **107,** 285 (1973).
52. R.M. Housley, U. Gonser, and R.W. Grant, *Phys. Rev. Lett.* **20,** 1279 (1968).
53. M.C.D. Ure and P.A. Flinn, in *Mössbauer Effect Methodology,* I.J. Gruverman, ed., Plenum Press New York, 1971, Vol. 7.
54. R. Zimmermann and R. Doerfler, *J. Phys. (Paris)* **41,** C1-107 (1980).
55. T.C. Gibb, *J. Phys. C, Solid State Phys.* **7,** 1001 (1974).
56. V.I. Goldanskii, E.F. Makarov, I.P. Suzdalev, and I.A. Vinogradov, *Sov. Phys. JETP* **31,** 407 (1970).